Online-Journals.org

iJOE International Journal of Online and Biomedical Engineering

iJOE | eISSN: 2626-8493 | Vol. 20 No. 11 (2024) | OPEN ACCESS

https://doi.org/10.3991/ijoe.v20i11.48029

PAPER

Estimate the Region of Interest, Movement and Magnitude of Ciliary Beat with Dense Optical Flow

Muhammad Daffa Khairi[1], Bedy Purnama[1](✉), Kosuke Imamura[2], Abo Miki[3]

[1]School of Computing, Telkom University, Bandung, Indonesia

[2]School of Electrical, Information and Communication Engineering, Kanazawa University, Kanazawa, Japan

[3]School of Medical, Pharmaceutical and Health Sciences, Kanazawa University Hospital, Kanazawa, Japan

bedypurnama@telkomuniversity.ac.id

ABSTRACT

In this study, we analyze mucociliary transport (MCT) by measuring the magnitude and identifying regions of ciliary beats using high-frame-rate microscopic videos. Our methodology, integrating dense optical flow (DOF), connected component labeling (CCL), Butterworth filter, and Fast Fourier Transform (FFT), captures ciliary movement and magnitude. We focus on region extraction, quantification of ciliary activity, and classification of power and recovery strokes in ciliary beat frequency (CBF), which are crucial for evaluating MCT efficiency. Our approach was able to extract the ciliary region semi-automatically, obtain the CBF, and visualize the ciliary movement in each frame. Despite dataset challenges and limited ground truth, our approach shows a promising result for ciliary dynamics research and medical diagnostics. We hope for future open-source datasets with ground-truth ciliary beat patterns to enable developing and evaluating automated ciliary analysis techniques, leading to improved assessment.

KEYWORDS

ciliary beat frequency (CBF), dense optical flow (DOF), Fast Fourier Transform (FFT)

1 INTRODUCTION

1.1 Research background

The respiratory system in our body has an effective waste disposal system to catch unknown particles and throw them out of our respiratory system because of the synchronized movement of cilia [1]. The movement speed of cilia depends on ciliary beat frequency (CBF) [2].

Ciliary beat frequency can be a parameter to diagnose a particular disease, such as primary ciliary dyskinesia (PCD). A new study indicates that the movement pattern of CBF can be essential proof to confirm a PCD patient because the ciliary are beating in a dyskinetic way when they try to maintain their regular beating frequency [3].

Optical flow is a technique to calculate and analyze the movement inside a video. It will try to compare two different frames consecutively based on their pixel

Khairi, M.D., Purnama, B., Imamura, K., Miki, A. (2024). Estimate the Region of Interest, Movement and Magnitude of Ciliary Beat with Dense Optical Flow. *International Journal of Online and Biomedical Engineering (iJOE)*, 20(11), pp. 66–79. https://doi.org/10.3991/ijoe.v20i11.48029

Article submitted 2024-01-17. Revision uploaded 2024-05-12. Final acceptance 2024-05-13.

intensity. This process results in a motion vector representing the pixel movement in the x and y coordinates [4].

Fourier transform is an integral transformation technique to redefine a function into two different domains, such as transforming a frequency domain into a time domain or otherwise [5]. This technique helps find the CBF of ciliary movement [1].

Several studies have employed optical flow and Fourier transform to extract the CBF from videos [2], [6], [7]. However, most of these approaches lack the ability for semi-automatic region of interest (ROI) extraction and rely on manual selection. Our method addresses this limitation by automatically extracting the ciliary movement region. Furthermore, it can obtain the CBF, differentiate between the power and recovery strokes of cilia movement, and estimate the overall cilia motion. We believe that, with a sufficiently large dataset, the motion vector data obtained from ciliary movement holds promise for further research. This includes exploring the possibility of predicting PCD based on the movement characteristics of cilia, as many studies solely focus on CBP and CBF as contributing factors [8], [9], [10].

1.2 Purpose

This study seeks to improve the estimation of ciliary regions, ciliary movements, and their magnitude by utilizing dense optical flow (DOF) for motion vector analysis. This approach allows for precise visualization and extraction of ciliary regions. The study focuses on identifying ciliary regions, determining their beating frequency, distinguishing between the power and recovery strokes of ciliary movement, and visualizing their motion. To support the analysis, connected component labeling (CCL) is used to label the identified ciliary regions within the algorithm. Additionally, a Butterworth filter is employed to remove noise from the motion vector signal, while FFT is applied to obtain the CBF and differentiate between the power and recovery strokes.

1.3 Limitation

Our main objective is to study the respiratory epithelial cells extracted from the bronchial wall of the patient. For this purpose, we will concentrate solely on the video sample “C0022.avi.” The cells were isolated and then suspended on a heated stage at a temperature of 37°C.

2 MATERIALS AND METHODS

2.1 Ciliary beat video

In our study, we examined a video sample provided by Kanazawa University in Japan for research purposes. The analysis will be conducted from a top-down perspective, focusing on a patient condition labeled as a physically unimpaired individual [1]. This study, including the video analysis, was conducted in accordance with the Declaration of Helsinki and approved by the Kanazawa University Ethical Review Committee (Approval No. 2018-149/12-19-2018) [1].

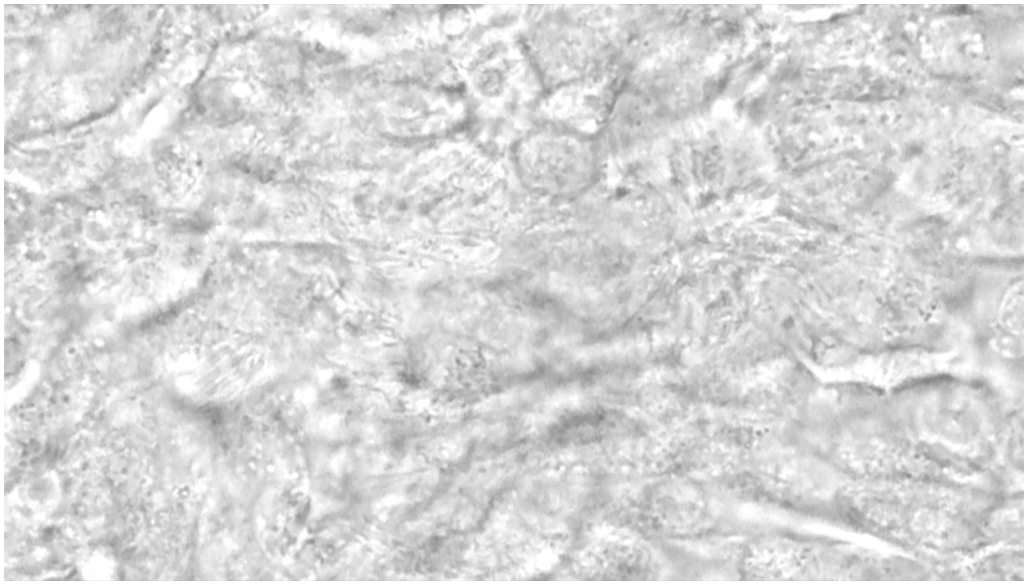

Fig. 1. A captured frame from the video we will analyse

Notes: This video was captured from the top-side perspective. This video is about respiratory epithelial cells taken from the patient's bronchial wall. The cells were suspended and placed on a heated stage at 37°C.

In Figure 1 shows the video example we analyzed, captured using high-speed video microscopy and an ×100 oil immersion objective lens of a light microscope (IX73 OLYMPUS). The footage, shot at 480 fps using a digital camera (DSC-RX100M6 Sony) with the lens appressed onto the microscope eyepiece and later slowed to 30 fps, comprises 512 frames, spans 1.0667 sec, and has a resolution of 1418 × 800.

2.2 Dense optical flow

In our study, we utilize the DOF technique, which differs from sparse optical flow (SOF) in its approach to motion vector calculation. DOF analyzes every pixel in a frame to determine motion vectors between sequential frames, unlike SOF, which tracks specific features such as edges and corners [11]. We use DOF due to its ability to track more minor details, such as the ciliary size in our videos, which SOF might struggle with due to its focus on more prominent, distinct features and its sensitivity to movement noise [12]. For a detailed understanding of DOF's workings, see Figure 2.

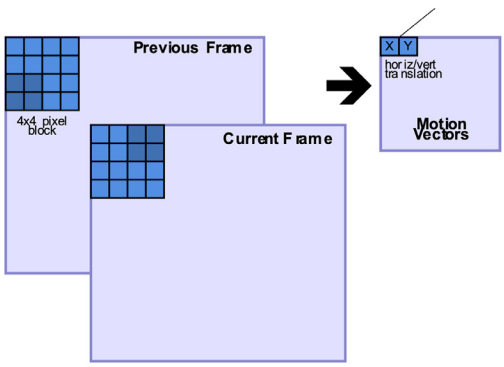

Fig. 2. Dense Optical Flow compares pixel intensity between two consecutive frames to generate a motion vector showing the magnitude of pixel movement in the x and y directions

Source: docs.nvidia.com.

2.3 Connected component labeling

Connected component labeling is an algorithm for detecting, counting, and segmenting corresponding regions in a binary image, which is particularly useful in identifying and quantifying ciliary beat regions in videos [3], [13]. By leveraging motion vector data, we are able to differentiate between ciliary and non-ciliary areas by representing the motion vector values in binary (see Figure 3).

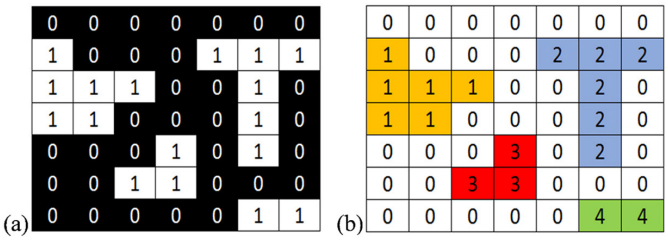

Fig. 3. (a) An example of a binary image before CCL was done (b) An example after CCL was done on the binary image

Source: cse.buffalo.edu.

2.4 Butterworth filter

The Butterworth filter is utilized in our research for its ability to fine-tune the sharpness of the filter's transition from passband to stopband, enabling a smooth transition without ringing artifacts [14]. This characteristic provides precise control over the filter's frequency response, which is important for the integrity and clarity of our signal processing needs. The Butterworth filter facilitates the meticulous and controlled approach required in our analysis, with its clean and gradual cutoff enhancing the accuracy and reliability of our results. Figure 4 illustrates the gain response of Butterworth low-pass filters.

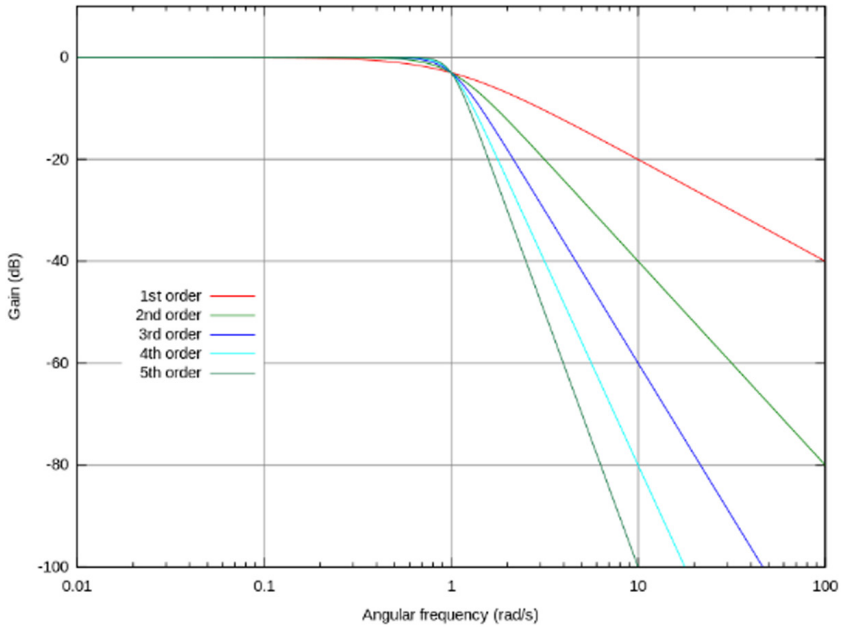

Fig. 4. An example of the gain response of Butterworth low-pass filters of orders 1 to 5 with a cut-off frequency of 1 rad/s. Gain is normalized to 0 dB in the pass band

Source: commons.wikimedia.org.

2.5 Fast Fourier Transform

Fast Fourier Transform (FFT) is a mathematical technique that converts a signal from its original domain to a frequency domain representation. This method was employed in our study to extract the CBF from ciliary movement [1], [15], and [16]. By analyzing the signal's frequency domain, FFT identifies the frequency with the peak amplitude corresponding to the CBF. Figure 5 shows how FFT works.

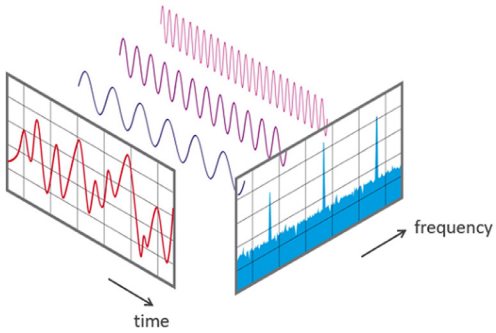

Fig. 5. A visualization of how FFT work to transform a signal into frequency domain representation
Source: medium.datadriveninvestor.com.

2.6 Ciliary beat frequency

Cilia are tiny hairs that line the surface of the cells in the airways. They move in a synchronized pattern to transport mucus and foreign particles out of the lungs [17]. This process is called mucociliary clearance, and it is a vital defense mechanism for the respiratory system [1], [18]. The rate at which the cilia move is called CBF, and it depends on various factors such as temperature, humidity, and exposure to drugs and noxious stimuli. CBF is important for maintaining healthy lungs and preventing infections and diseases that can affect the respiratory epithelium. In one CBF cycle, there is a power and recovery stroke. During the power stroke, the cilium moves approximately as a straight rod, and during the recovery stroke, it rolls close to the surface in a tangential motion. The power stroke encounters strong viscous resistance and generates thrust, whereas the recovery stroke returns the cilium to its starting position while avoiding viscous resistance [19], [20]. In terms of movement speed, the power stroke is faster than the recovery stroke [21], [22]. See Figure 6 for an example of cilia structure.

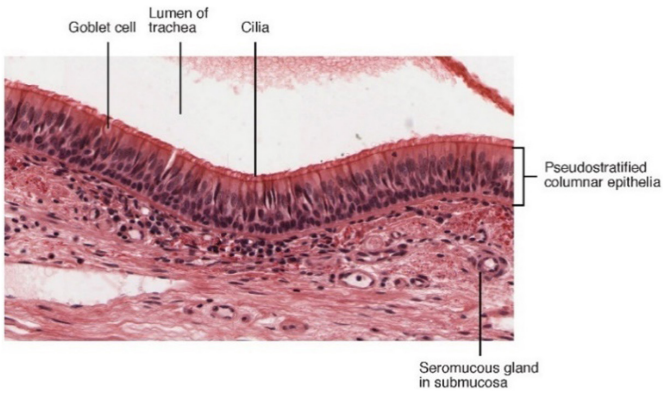

Fig. 6. The movement of cilia is driven by tiny molecular motors called dynein. It does this by making nearby microtubules move along each other and create force
Source: openstax.org.

2.7 Pipeline process

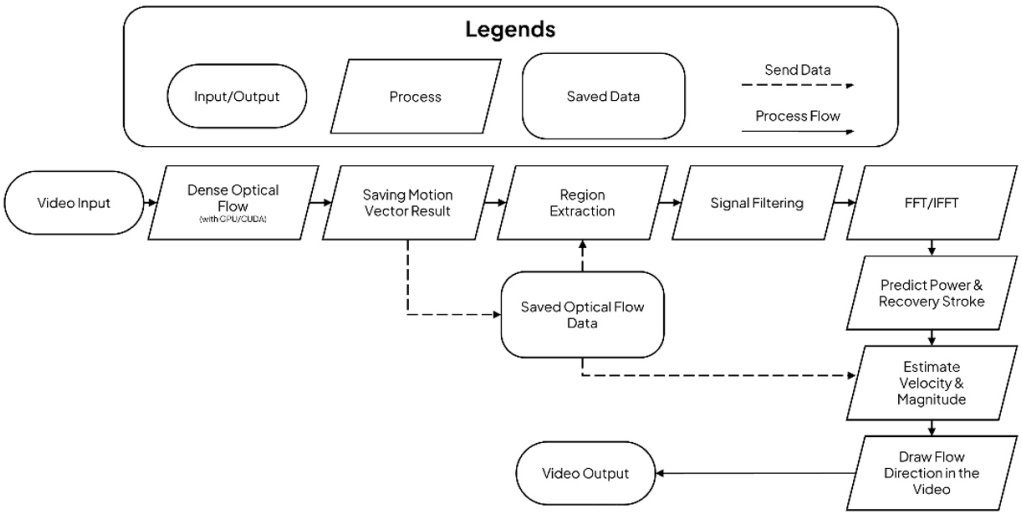

Fig. 7. Pipeline process

Notes: For our DOF calculations, we utilize an NVIDIA RTX 3060 Mobile GPU with 6GB GDDR6 VRAM. It able to compute DOF in nearly real-time, significantly faster than using CPU.

Video preprocessing. Each frame in the video has an RGB color channel. To make it easier for DOF to process and get the motion vector result, we transform the RGB color channel into a grayscale color channel. This is because the DOF only perceives the difference in the pixel intensity in each frame. Hence the use of RGB channel is wasted here.

Motion vector. Our approach meticulously computes motion vectors for each frame in a video sequence using the Gunnar Farneback DOF algorithm from the OpenCV Python library, specifically through the "cv2.calcOpticalFlowFarneback" function. We leverage the enhanced functionalities of the OpenCV-contrib module to expedite these computations with the power of GPU/CUDA cores. Table 1 shows the parameter we used for dense optical flow.

Table 1. Parameter configuration of "cv2.calcOpticalFlowFarneback"

Parameter	Value
prev	*prev_gray*
next	*gray*
flow	*None*
pyr_scale	0, 5
levels	3
winsize	15
iterations	3
poly_n	5
poly_sigma	1, 2
flags	0

Upon completing the DOF process, we obtain the motion vector results for each frame. Given the importance of these motion vector results for subsequent

procedures, employing an effective data structure for their storage and retrieval is essential. Figure 8 shows the data structure we used to save the motion vector result.

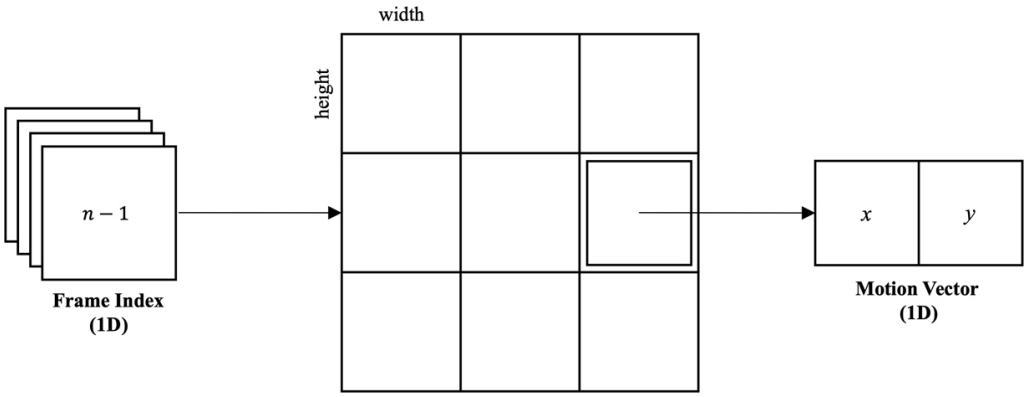

Fig. 8. 4D dimension array, where the motion vector result will be saved

Region extraction. The parameter for thresholding is based on the percentile range of motion vectors, and candidate region selection is based on size criteria based on the labelled region candidate.

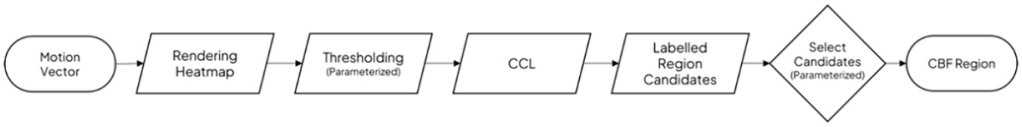

Fig. 9. Parameter for thresholding and candidate region selection criteria

The analysis extends to pinpointing ciliary regions by examining the motion vector data to gauge pixel movements (see Figure 9). These regions are then visualized using a heatmap. Given the variable nature of ciliary motion, which complicates the determination of CBF, we selectively concentrate on optimal regions based on specific heatmap values. The heatmap representation was based on motion vector data from the first frame until the last frame of the video. Then we binarize these regions by thresholding, converting values from the heatmap into binary to aid in labeling through CCL [13]. After each region has been labeled through CLL, we crafted an algorithm that semi-automatically choose the ideal region based on the given parameter (see Figure 10).

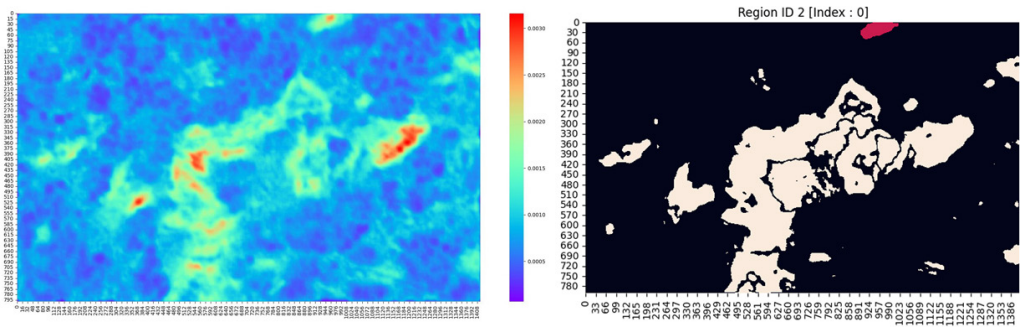

Fig. 10. (Left). Heatmap visualization of motion vector data, highlighting the pixel movement based on the sum of motion vector data from the first frame until the last frame. (Right). Resultant binary image after applying CCL to the heatmap data, with selected ciliary regions labelled for further analysis in determining CBF

Obtain CBF. We will use the previously saved motion vector data to make a new data named "Delta" data. Delta data will represent how big the difference between the current frame and the previous frame motion vector (the x and y magnitude) results in the selected region.

To enhance the quality and diminish noise interference, we implement a 5th-order lowpass Butterworth filter on the delta data by deploying the "signal.butter" function from the SciPy library, with a normalized cutoff frequency (Wn) of 3800/75000, sampling rate (fs) of 75000 Hz, and an order of 5. This step is crucial for preparing the data for frequency analysis. Following the noise reduction, we apply the "fft.fft" function from the NumPy library to perform a FFT on the filtered data, which aids in identifying the preliminary CBF [15], [23].

Aware that these initial frequencies may not accurately represent the ciliary motion, we proceed with a meticulous selection process to isolate the actual CBF frequencies. For the final step, we employ the "fft.ifft" function for an inverse Fast Fourier Transform (IFFT), enabling us to reconstruct a time-domain signal that more accurately captures the intrinsic motion of the cilia, free from the distortions of noise. The outcome of this refined process is visualized in the CBF movement graph post-IFFT, providing a clear and precise depiction of the ciliary dynamics. Figure 11 shows the result of our signal processing pipeline proposed in Figure 7.

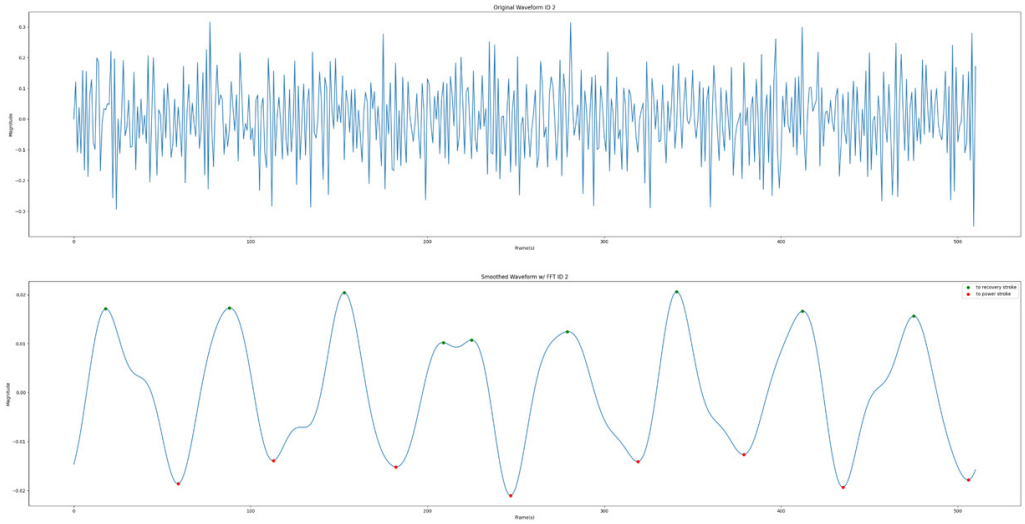

Fig. 11. (Top) Original waveform depicting Delta data with inherent noise and fluctuations before any filtering (Bottom) Processed waveform post-Butterworth filter application, FFT, selective frequency isolation, and IFFT, which includes identified peaks and valleys

Our analysis discerns two predominant ciliary movements: the rapid power stroke, driven by intense viscous resistance creating thrust, and the slower recovery stroke, which aims to evade such resistance [19]. Through the CBF movement graph, we identify peaks and troughs and then differentiate them into two distinct graph categories: power strokes and recovery strokes. We determine the nature of each stroke by comparing the magnitudes of these categories, with the higher magnitude indicating a power stroke and the lower indicating a recovery stroke [21], [22]. See Figure 12 for the final result of region extraction, Figure 13 for the CBF pattern from Region ID 2 (see Figure 12 for region reference), Figure 14 for the ciliary movement flow result, and Table 3 for the CBF result.

3 RESULTS

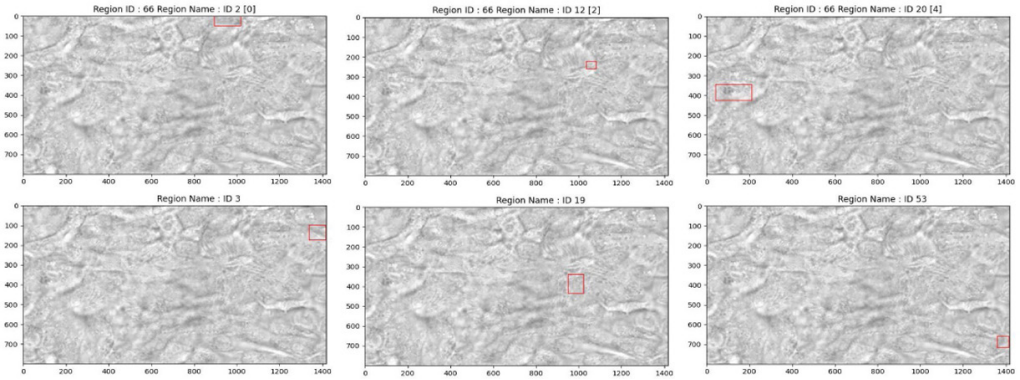

Fig. 12. Selected ciliary beat areas that has been identified from the region extraction process

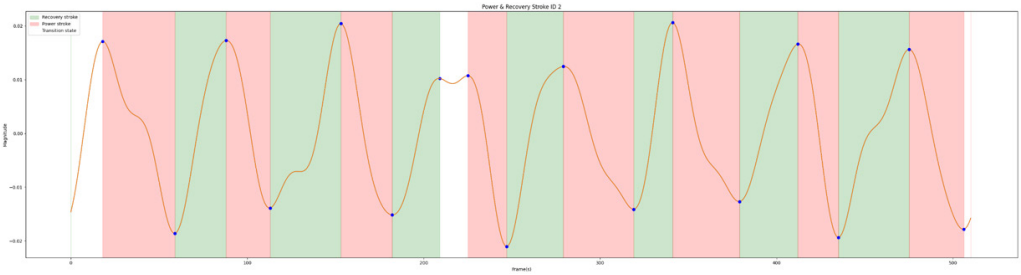

Fig. 13. CBF movement graph (Region ID 2)

Figure 13 shows the CBF movement graph (Region ID 2) highlighting red regions for power strokes with higher magnitudes and green for recovery strokes with subdued motion. Blue dots mark the peaks and valleys, outlining the ciliary motion cycle. Refer to Table 2 for detailed measurement.

Table 2. The magnitude of captured CBF in region ID 2

No	Stroke Type	Start Frame	End Frame	Magnitude
1	Power	18	59	0.0357
2	Recovery	59	88	0.0359
3	Power	88	113	0.0312
4	Recovery	113	153	0.0343
5	Power	153	182	0.0356
6	Recovery	182	209	0.0254
7	Power	225	247	0.0318
8	Recovery	247	279	0.0335
9	Power	279	319	0.0266
10	Recovery	319	341	0.0347
11	Power	341	379	0.0333
12	Recovery	379	412	0.0293

(*Continued*)

Table 2. The magnitude of captured CBF in region ID 2 (*Continued*)

No	Stroke Type	Start Frame	End Frame	Magnitude
13	Power	412	435	0.0360
14	Recovery	435	475	0.0350
15	Power	475	506	0.0335
Result	**Total Power Stroke**		8	
	Total Recovery Stroke		7	
	Crop Coordinate	((895, 0), (1019, 50))		

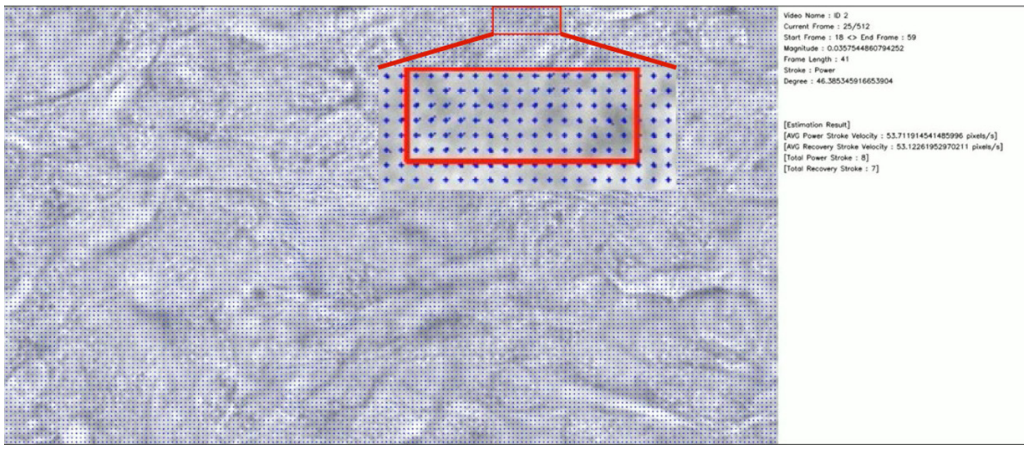

Fig. 14. The video frame sample result for Region ID 2

In Figure 14, the red box area is the current inspected region. The texts on the right side are the information about what is going on in that region. We can also see the cilia's movement at every frame (highlighted by the red colour box).

Table 3. The CBF results from all extracted regions from the video sample

Average (Hz)	Standard Deviation (Hz)	Minimum (Hz)	Maximum (Hz)
9.0	3.5	4.5	15.5

4 DISCUSSION

In the discussion of our research, we successfully employed DOF to determine the region of interest, visualize its movement and magnitude of ciliary beat, based on the motion vectors. When classifying the type of ciliary movement—whether a power or recovery stroke—we relied solely on the magnitude of the movement, a methodological choice dictated by the top perspective of the video footage. Figure 15 show an illustration of power and recovery stroke moved from its side and top view. However, we only focus on distinguishing them by using the estimation of CBF movement magnitude.

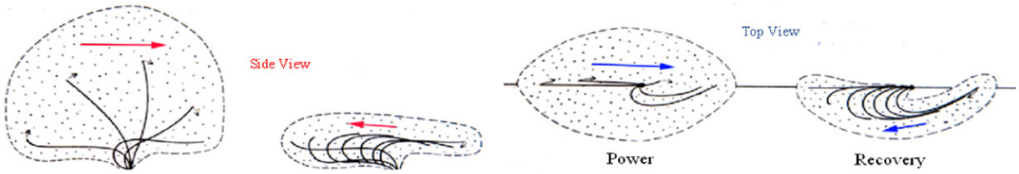

Fig. 15. A visualization of power and recovery stroke magnitude
Source: researchgate.net.

In our investigation into identifying the dominant CBF, anticipated to fall within the 3–30 Hz range, we encounter the inherent challenge of validation in the absence of definitive ground truth and comparable datasets. At the moment of our research, the majority of available open-source datasets and studies feature samples obtained through nasal brushing, which could introduce a variance from our bronchial specimens [9], [24]. Further studies are needed.

Our assistant professor, who specializes in the respiratory medicine field, further illuminates the complexity of comparing CBF values across studies, noting that CBF values can significantly vary based on measurement conditions. For instance, our measuring system shows a decrease in CBF when observed with a 100× objective lens compared to a 40× lens, possibly due to pressure applied during observation with the higher magnification lens. We suggest that a more robust comparison might be achieved through the analysis of the same video using different measurement methods, such as visual assessment or alternative algorithms [1]. This approach underscores the necessity of employing multiple methods to compare CBF values accurately, highlighting the limitations of relying solely on measurements from a single video for comprehensive analysis.

5 CONCLUSION

Our study has effectively demonstrated the capability to extract the ciliary region from video data, quantify its beating magnitude, distinguish between power and recovery strokes, and visualize its movement. This achievement was realized through the application of DOF for capturing motion vectors of cilia, generating movement heatmaps to visualize activity, using CCL to label the extracted ciliary region, and utilizing Butterworth filtering to minimize noise, thus refining motion vector data and later being used with FFT to accurately determine CBF. Our approach, although challenged by the absence of definitive ground truth and variability in data sources, underscores the importance of employing a multifaceted analysis technique. The discussion highlighted the necessity of employing diverse measurement methods to overcome the variability introduced by different observational conditions, such as magnification differences, which affect CBF readings.

6 ACKNOWLEDGMENT

We acknowledge Telkom University, Kanazawa University, and Kanazawa Hospital University for their collaboration in this research. Special thanks are due to Kanazawa Hospital University for providing the dataset. We confirm that there are no conflicts of interest among the authors or the participating institutions.

7 REFERENCES

[1] M. Abo *et al.*, "Comparing region of interest selection and whole-field analysis for measurement of ciliary beat frequency in high-speed video analysis," *Respir. Investig.*, vol. 62, no. 3, pp. 419–425, 2024. https://doi.org/10.1016/j.resinv.2024.02.016

[2] M. Figl, M. Lechner, T. Werther, F. Horak, J. Hummel, and W. Birkfellner, "Automatic analysis of ciliary beat frequency using optical flow," in *Medical Imaging 2012: Image Processing*, 2012, vol. 8314, p. 831453. https://doi.org/10.1117/12.911616

[3] L. He, X. Ren, Q. Gao, X. Zhao, B. Yao, and Y. Chao, "The connected-component labeling problem: A review of state-of-the-art algorithms," *Pattern Recognit.*, vol. 70, pp. 25–43, 2017. https://doi.org/10.1016/j.patcog.2017.04.018

[4] C. M. Smith *et al.*, "ciliaFA: A research tool for automated, high-throughput measurement of ciliary beat frequency using freely available software," *Cilia*, vol. 1, no. 14, 2012. https://doi.org/10.1186/2046-2530-1-14

[5] A. Rizal, W. Priharti, and S. Hadiyoso, "Seizure detection in epileptic EEG using short-time fourier transform and support vector machine," *International Journal of Online and Biomedical Engineering*, vol. 17, no. 14, pp. 65–78, 2021. https://doi.org/10.3991/ijoe.v17i14.25889

[6] E. Parrilla *et al.*, "Primary ciliary dyskinesia assessment by means of optical flow analysis of phase-contrast microscopy images," *Computerized Medical Imaging and Graphics*, vol. 38, no. 3, pp. 163–170, 2014. https://doi.org/10.1016/j.compmedimag.2013.12.010

[7] E. Parrilla *et al.*, "Ciliary motility activity measurement using a dense optical flow algorithm," in *2013 35th Annual International Conference of the IEEE Engineering in Medicine and Biology Society (EMBC)*, Osaka, Japan, 2013, pp. 4446–4449. https://doi.org/10.1109/EMBC.2013.6610533

[8] W. De Jesús-Rojas *et al.*, "Advancing primary ciliary dyskinesia diagnosis through high-speed video microscopy analysis," *Cells*, vol. 13, no. 7, p. 567, 2024. https://doi.org/10.3390/cells13070567

[9] P. Sampaio *et al.*, "CiliarMove: New software for evaluating ciliary beat frequency helps find novel mutations by a Portuguese multidisciplinary team on primary ciliary dyskinesia," *ERJ Open Res.*, vol. 7, no. 1, 2021. https://doi.org/10.1183/23120541.00792-2020

[10] J. Raidt *et al.*, "Ciliary beat pattern and frequency in genetic variants of primary ciliary dyskinesia," *European Respiratory Journal*, vol. 44, no. 6, pp. 1579–1588, 2014. https://doi.org/10.1183/09031936.00052014

[11] O. Zvorișteanu, S. Caraiman, and V.-I. Manta, "Speeding up semantic instance segmentation by using motion information," *Mathematics*, vol. 10, no. 14, p. 2365, 2022. https://doi.org/10.3390/math10142365

[12] T. X. B. Nguyen, K. Rosser, and J. Chahl, "A comparison of dense and sparse optical flow techniques for low-resolution aerial thermal imagery," *J. Imaging*, vol. 8, no. 4, p. 116, 2022. https://doi.org/10.3390/jimaging8040116

[13] C. Fatichah, J. L. Buliali, A. Saikhu, and S. Tena, "A hybrid fuzzy morphology and connected components labeling methods for vehicle detection and counting system," *International Journal on Smart Sensing and Intelligent Systems*, vol. 9, no. 2, pp. 765–779, 2016. https://doi.org/10.21307/ijssis-2017-894

[14] N. F. Rabbi, "Design, implementation, comparison, and performance analysis between analog Butterworth and Chebyshev-I low pass filter using approximation, python and proteus," *arXiv*, no. 2102.09048, 2021. https://doi.org/10.48550/arXiv.2102.09048

[15] V. Renò, M. Sciancalepore, G. Dimauro, R. Maglietta, M. Cassano, and M. Gelardi, "A novel approach for the automatic estimation of the ciliated cell beating frequency," *Electronics*, vol. 9, no. 6, p. 1002, 2020. https://doi.org/10.3390/electronics9061002

[16] T. Najafi, R. Jaafar, R. Remli, W. A. W. Zaidi, and K. Chellappan, "Brain dynamics in response to intermittent photic stimulation in epilepsy," *International Journal of Online and Biomedical Engineering (iJOE)*, vol. 18, no. 5, pp. 80–95, 2022. https://doi.org/10.3991/ijoe.v18i05.27647

[17] J. C. Jing, J. J. Chen, L. Chou, B. J. F. Wong, and Z. Chen, "Visualization and detection of ciliary beating pattern and frequency in the upper airway using phase resolved doppler optical coherence tomography," *Sci. Rep.*, vol. 7, p. 8522, 2017. https://doi.org/10.1038/s41598-017-08968-x

[18] M. B. Antunes and N. A. Cohen, "Mucociliary clearance – a critical upper airway host defense mechanism and methods of assessment," *Curr. Opin. Allergy and Clin. Immunol.*, vol. 7, no. 1, pp. 5–10, 2007. https://doi.org/10.1097/ACI.0b013e3280114eef

[19] S. Gueron and K. Levit-Gurevich, "Energetic considerations of ciliary beating and the advantage of metachronal coordination," *Proc. Natl. Acad. Sci.*, vol. 96, no. 22, pp. 12240–12245, 1999. https://doi.org/10.1073/pnas.96.22.12240

[20] M. Yasuda *et al.*, "Intracellular Cl^- regulation of ciliary beating in ciliated human nasal epithelial cells: Frequency and distance of ciliary beating observed by high-speed video microscopy," *Int. J. Mol. Sci.*, vol. 21, no. 11, p. 4052, 2020. https://doi.org/10.3390/ijms21114052

[21] S. A. Baba, "Regular steps in bending cilia during the effective stroke," *Nature*, vol. 282, pp. 717–720, 1979. https://doi.org/10.1038/282717a0

[22] F. Ijaz and K. Ikegami, "Live cell imaging of dynamic behaviors of motile cilia and primary cilium," *Microscopy*, vol. 68, no. 2, pp. 99–110, 2019. https://doi.org/10.1093/jmicro/dfy147

[23] R. Fradique *et al.*, "Assessing motile cilia coverage and beat frequency in mammalian in vitro cell culture tissues," *R. Soc. Open. Sci.*, vol. 10, no. 8, 2023. https://doi.org/10.1098/rsos.230185

[24] M. A. K. Olm, J. E. Kögler, M. Macchione, A. Shoemark, P. H. N. Saldiva, and J. C. Rodrigues, "Primary ciliary dyskinesia: Evaluation using cilia beat frequency assessment via spectral analysis of digital microscopy images," *J. Appl. Physiol.*, vol. 111, no. 1, pp. 295–302, 2011. https://doi.org/10.1152/japplphysiol.00629.2010

8 AUTHORS

Muhammad Daffa Khairi earned a Bachelor of Computer Science in Informatics Engineering from Telkom University, Bandung, Indonesia, in 2024. His interests are machine learning, deep learning, image and video processing, and software development (E-mail: ihsbiasa@telkomuniversity.ac.id).

Bedy Purnama earned a Bachelor of Science degree in Physics from Bandung Institute of Technology, Indonesia, in 2003. Later, in 2018, he earned a Master of Engineering degree in Electrical Engineering from the same institution. In 2021, he earned a Ph.D. in the Division of Electrical Engineering and Computer Science at Kanazawa University, Japan. Since 2010, he has held a permanent position as a lecturer in the School of Computing at Telkom University, Indonesia. The primary areas of his research include image processing, machine learning, and computer vision (E-mail: bedypurnama@telkomuniversity.ac.id).

Kosuke Imamura earned his academic degrees from Kanazawa University, Japan. He served as an assistant professor from 2000 to 2005 and then as a lecturer from 2005 to 2010. Since 2010, he has been an Associate Professor at the Institute of Science and Engineering, Kanazawa University. His research interests include image processing, video processing, and related areas. He is actively involved in academic

societies such as the Information Processing Society of Japan and the Institute of Electronics, Information, and Communication Engineers (E-mail: imamura@ec.kanazawa-u.ac.jp).

Abo Miki is a researcher and clinician affiliated with Kanazawa University, Japan. She has contributed to studies in respiratory medicine, focusing on pulmonary diseases such as asthma and chronic obstructive pulmonary disease (COPD). Abo's research includes investigating the prevalence and clinical features of asthma-COPD overlap (ACO) and examining exhaled nitric oxide levels in patients with atopic cough and cough variant asthma. Her work aims to improve the understanding and management of respiratory conditions (E-mail: abomiki@staff.kanazawa-u.ac.jp).